J|A|C|S ARTICLES

Published on Web 07/06/2009

# Synthesis and Characterization of $Na_5M_{2+x}Sn_{10-x}$ ($x \approx 0.5$, M = Zn, Hg)—A Doped Tetrahedral Framework Structure

Siméon Ponou, Sung-Jin Kim, and Thomas F. Fässler*

*Department Chemie der Technischen Universität München, Lichtenbergstrasse 4, D-85747 Garching, Germany*

Received April 3, 2009; E-mail: thomas.faessler@lrz.tum.de

***Abstract:*** Two homologous and isostructural compounds $Na_5M_{2+x}Sn_{10-x}$ (M = Zn, Hg) were obtained by direct reaction of the elements at high temperature. The crystal structures of these novel phases were determined from single-crystal X-ray diffraction data and represent a new structure type in tin chemistry. They crystallize in the space group *Pbcn* (No. 60, $Z = 4$) with $a = 12.772(1)$, $b = 10.804(1)$, and $c = 12.777(1)$ Å, $V = 1763.1(2)$ Å$^3$ for $Na_5Zn_{2.28}Sn_{9.72(2)}$ (**I**) and $a = 12.958(1)$, $b = 10.984(1)$, and $c = 12.960(1)$ Å, $V = 1844.5(2)$ Å$^3$ for $Na_5Hg_{2.39}Sn_{9.61(1)}$ (**II**). The structures consist of an anionic 3D open framework of tetrahedrally coordinated Sn and M atoms interwoven with a cationic 2D array of interconnected $\{NaNa_4\}$ tetrahedra. The framework can be partitioned into fragments of realgar-like units $\{Sn_{8-x}M_x\}^{2x-}$ and twice as many $\{Sn-M\}^{2-}$ dimers. Formally, the compounds are charge-balanced Zintl phases for $x = 0.5$. As the structure refinements lead to $x = 0.28$ and 0.39 for **I** and **II**, respectively, both structures are electron-rich and expected to be metallic. Theoretical investigations at the density functional theory level reveal a deep minimum at the Fermi level for $x = 0.5$. According to rigid band analyses, the electronic structure of the phases with the experimentally observed compositions corresponds to heavily doped semiconductors, thereby meeting an important requirement of thermoelectric materials.

## 1. Introduction

The most common crystal structure adopted by many commercial semiconductors is the diamond and sphalerite structure, in which each atom is tetrahedrally coordinated by strong covalent bonds to four adjacent atoms. Elemental Si and Ge (and α-Sn) are archetypal band gap compounds with diamond structure. Moreover, the isoelectronic III−V binary compounds, which adopt the sphalerite structure, are the most frequently used semiconductors, with GaAs being the most prominent commercially used representative. There is also a large number of Zintl phases with a diamond-like substructure, such as the prominent NaTl,[1] which is the simplest filled variant of the diamond structure, where the Na atoms themselves also form a diamond-type structure. In this view, the NaTl structure can be understood as a penetration of two diamond lattices, $^3_\infty$[Tl] and $^3_\infty$[Na]. In analogy to the relationship between the diamond and sphalerite structures, ternary ordered variants such as $Li_2ZnSn$[2] exist. In the anionic $[ZnSn]^{2-}$ framework of the latter, each Sn atom is tetrahedrally coordinated by Zn atoms and *vice versa*. The closely related half-Heusler (HH) compounds (ATE), like ZrNiSn[3] or YNiSb, consist of an electropositive metal A, a late transition metal T, and a heavy main-group atom E of group 14 or 15. Here, the ionic three-dimensional framework features a cubic close-packed (ccp) arrangement of E atoms, with the T atoms located in 50% of the tetrahedral voids. The atoms T and E form a sphalerite lattice, which becomes a diamond lattice if T = E. The A atoms are located in the octahedral voids of the ccp arrangement. Hence, the HH structure is another cation-stuffed version of the sphalerite structure. Semiconducting HH compounds form an interesting family, including the most promising classes of thermoelectric materials.[5,6] Qualitatively, the semiconducting properties of most HH compounds have been understood by noting that the 18-electron count for T atoms implies a closed-shell electron configuration (*i.e.*, $d^{10} + s^2 + p^6$),[7,8] and their electronic structures are described according to the Zintl−Klemm concept as $A^{n+}(TE)^{n-}$. The HH materials display respectable thermopower and electrical conductivity, which lead to a large power factor required for effective energy conversion. However, due to their simple isotropic crystal structure based on the ccp arrangement of atoms, their thermal conductivities $\kappa_L$ are fairly large.[5,6] Hence, intense research efforts have been dedicated to the synthesis of open-framework compounds containing the chemical and electronic features of the HH materials, but in which a more complex structure may induce a dip in the $\kappa_L$.[6]

(1) (a) Zintl, E.; Woltersdorf, G. *Z. Electrochem.* **1935**, *41*, 876. (b) Christensen, N. E. *Phys Rev. B* **1985**, *32*, 207. (c) Schmidt, P. C. *Struct. Bonding (Berlin)* **1987**, *65*, 91.
(2) (a) Schuster, H. U. *Naturwissenschaften* **1966**, *53*, 361. (b) Pobitschka, W.; Schuster, H. U *Z. Naturforsch.* **1978**, *B33*, 115.
(3) Eberz, U.; Seelentag, W.; Schuster, H. U. *Z. Naturforsch.* **1980**, *B35*, 1341.
(4) Dwight, A. E. *Proc. Rare Earth Res. Conf.* **1974**, 11.
(5) *Thermoelectric Materials 2000*; Tritt, T. M., Nolas, G. S. Mahan, G., Kanatzidis, M. G., Mandrus, D., Eds.; MRS Symposium Proceedings No. *626*; Materials Research Society: Pittsburgh, 2000.
(6) Larson, P.; Mahanti, S. D.; Salvador, J.; Kanatzidis, M. G. *Phys. Rev. B* **2000**, *74*, 035111.
(7) (a) Jung, D.; Koo, H.-J.; Whangbo, M.-H. *J. Mol. Struct. (THEOCHEM)* **2000**, *527*, 113. (b) Galanakis, I.; Dederichs, P. H.; Papanikilaou, N. *Phys. Rev. B* **2002**, *66*, 134428.
(8) Kandpal, H. C.; Felser, C.; Seshadri, R. *J. Phys. D: Appl. Phys.* **2006**, *39*, 776.



**10.1021/ja902664c CCC: $40.75** 

Meanwhile, several alkali metal−tin binary phases with anionic tin substructures of various dimensionalities have been structurally characterized.[9] In $Li_5NaSn_4$, a two-dimensional partial structure of α-Sn is clearly visible.[10] In the Sn-rich region of the binary phase diagram, structures with polyanionic networks with various atom connectivities and bond types are observed. Two-dimensional tin networks are found in $Na_7Sn_{12}$[11] and $NaSn_2$,[12] and a three-dimensional open-tunnel tin network is present in $Na_5Sn_{13}$.[13] In the tin-richest phase $NaSn_5$,[14] both α- and β-Sn structural motifs are present. The structural diversity of the tin networks increases in ternary systems, *e.g.*, in $NaTrSn_2$ (Tr = Ga, In),[15,16] which has a unique zeolite-like structure with open tunnels. Moreover, in our recent papers, we demonstrated that the addition of group 12 metals like Zn into the Na−Sn system leads to compounds in which both the stannide and the trielide-like structural features are realized.[17]

Nevertheless, compounds with fully tetrahedrally coordinated framework atoms are rather rare in the field of polar intermetallic phases. Herein, we report the synthesis and characterization of the novel phases $Na_5M_{2+x}Sn_{10-x}$ ($x \approx 0.5$; M = Zn, Hg) with a unique framework of entirely four-fold-connected $d^{10}$ and p-block elements. The framework stuffed with Na atoms is structurally related to a partially filled diamond-type structure and thus HH materials. The new phases were obtained during the systematic investigation of the ternary systems A−Sn−M (A = alkali metal, M = group 12 metal).[17,18]

## 2. Experimental Section

**Synthesis.** The starting materials used for the synthesis were stored in an argon-filled glovebox: Sn granules (Chempur, 99.999%), Na (Merck, 99%), Zn granules (Merk, extra pure), and liquid Hg (Alfa Aesar, 99.0%). Stoichiometric amounts of these elements (total ∼1.2 g) were loaded into niobium ampules, which were sealed using an arc welder and enclosed in a quartz tube. After evacuation, the samples were heated to 600 °C at a rate of 2 K $min^{-1}$, held there for 24 h, and subsequently cooled to room temperature at a rate of 0.1 K $min^{-1}$. The products crystallize in the form of silvery block-shaped crystals that are moderately air- and moisture-sensitive at room temperature. Single crystals of good quality of the Zn phase $Na_5Zn_{2+x}Sn_{10-x}$ were first obtained as a product from a sample loaded as Na:Ca:Zn:Sn = 4:3:3:9, aiming to investigate the eventual Na-by-Ca substitution in the Na/Zn/Sn system; the byproducts in this reaction were β-NaSn and CaZnSn. In further reactions to optimize the synthesis, the compound was also obtained as a pure phase (based on powder XRD) in an attempt to prepare a pure phase of $Na_6ZnSn_2$.[18a] Quenching that sample (loading "$Na_6ZnSn_2$"; the hot ampule was dropped head-first into a bucket with liquid nitrogen) led to the removal of one end-cap and presumably to the removal of excess Na and Zn. The synthesis from stoichiometric loadings, using the above-mentioned heat treatment, leads to the title phase (>90 vol %) and small amounts of β-NaSn. Single-crystal data (below) came from those stoichiometric reactions. Single crystals of the Hg analogue were formed by using a Sn flux (2-fold excess) and stoichiometric amounts of Hg and Na. The product consists of the target phase $Na_5Hg_{2+x}Sn_{10-x}$ accompanied by elemental Sn.

***Table 1.*** Crystallographic Data for $Na_5Zn_{2.28}Sn_{9.72(2)}$ (**I**) and $Na_5Hg_{2.39}Sn_{9.61(1)}$ (**II**)

| | | |
|---|---|---|
| empirical formula | $Na_5Zn_{2.28}Sn_{9.72(2)}$ | $Na_5Hg_{2.39}Sn_{9.61(1)}$ |
| fw | 1417.66 | 1734.97 |
| *T*/K | 293(2) | |
| space group | *Pbcn* (No. 60) | |
| unit cell parameters/Å | $a = 12.772(1)$ | $a = 12.958(1)$ |
| | $b = 10.804(1)$ | $b = 10.984(1)$ |
| | $c = 12.777(1)$ | $c = 12.960(1)$ |
| unit cell volume/$Å^3$ | 1763.1(2) | 1844.5(2) |
| *Z* | 4 | |
| $\rho_{calc}$/g·$cm^{-3}$ | 5.34 | 6.25 |
| $\mu$/$mm^{-1}$ ($\lambda = 0.71073$ Å) | 16.64 | 32.66 |
| final *R* indices | $R_1 = 0.035/wR_2 = 0.069$ | $R_1 = 0.033/wR_2 = 0.076$ |
| final *R* indices (all data) | $R_1 = 0.048/wR_2 = 0.072$ | $R_1 = 0.047/wR_2 = 0.078$ |

**EDX Measurements.** Semiquantitative chemical analyses were carried out using a JEOL 5900LV electron microscope system operating at 20 kV and equipped with a Röntec detector system for EDX analysis. The bulk purities of the single crystals were independently confirmed, indicating the presence of only Na, Sn, and Zn (respectively Hg), and no other elements heavier than boron could be detected.

**X-ray Studies.** Several single crystals were selected in an argon-filled glovebox and mounted in a glass capillary which was subsequently sealed to prevent contact with air. Several crystals were checked by collecting data of a few frames, and non-twinned single crystals were used for full data collection at room temperature (Mo Kα radiation, graphite monochromator). All data were collected on an Oxford Xcalibur3 diffractometer with a CCD detector. A total of 776 frames were collected in four ω scans and one φ scan with 20 s exposure times for **I**, and four series of 138 frames were collected for **II** with an exposure time of 45 s. In both cases the crystal-to-detector distance was 50 mm. The reflections were collected over the range $2\theta_{max} = 55.5°$ and were corrected for absorption (empirical) using the program CrysAlis RED (Oxford Diffraction Ltd.). The two isotypic phases $Na_5M_{2+x}Sn_{10-x}$ (M = Zn, Hg) crystallize in the space group *Pbcn* (No. 60, $Z = 4$) with $a = 12.772(1)$, $b = 10.804(1)$, and $c = 12.777(1)$ Å for M = Zn (**I**) and $a = 12.958(1)$, $b = 10.984(1)$, and $c = 12.960(1)$ Å for M = Hg (**II**). The data were processed using the SHELXTL package,[19] solved by direct methods (SHELXS-97), and refined (on $F^2$) with SHELXL-97. Satisfactory residuals (all data) were obtained (for $Na_5Zn_{2.28}Sn_{9.72(2)}$ (**I**), $R_1 = 0.048$, $wR_2 = 0.072$; and for $Na_5Hg_{2.39}Sn_{9.61(1)}$ (**II**), $R_1 = 0.047$, $wR_2 = 0.078$). Relevant crystallographic and refinement details are listed in Table 1, and Table 2 contains selected interatomic distances. Further details of the crystal structure investigations can be obtained from the Fachinformationszentrum Karlsruhe, 76344 Eggenstein-Leopoldshafen, Germany (fax (+49) 7247-808-666; E-mail crysdata@fiz.karlsruhe.de) on quoting the depository numbers CSD-420536 (M = Zn) and CSD-420537 (M = Hg).

The phase analyses of the products by X-ray powder diffraction were done using a Stoe Stadi P2 diffractometer (Ge(111) monochromator for Cu $K\alpha_1$ radiation, $\lambda = 1.54056$ Å) equipped with a linear position-sensitive detector with $2\theta_{eff} \approx 40°$. For measure-


(9) Fässler, T. F. *Z. Anorg. Allg. Chem.* **2006**, *632*, 1125.
(10) Volk, K.; Müller, W. *Z. Naturforsch.* **1978**, *B33*, 598.
(11) Fässler, T. F.; Hoffmann, S. *Inorg. Chem.* **2003**, *42*, 5474.
(12) Dubois, F.; Schreyer, M.; Fässler, T. F. *Inorg. Chem.* **2005**, *44*, 477.
(13) Vaughey, J. T.; Corbett, J. D. *Inorg. Chem.* **1997**, *36*, 4316.
(14) Fässler, T. F.; Kronseder, C. *Angew. Chem., Int. Ed. Engl.* **1998**, *37*, 1571.
(15) Blase, W.; Cordier, G.; Kniep, R.; Schmidt, R. *Z. Naturforsch.* **1989**, *44b*, 505.
(16) Vaughey, J. T.; Corbett, J. D. *J. Am. Chem. Soc.* **1996**, *118*, 12098.
(17) Kim, S.-J.; Hoffmann, S. D.; Fässler, T. F. *Angew. Chem. Int. Ed* **2007**, *46*, 3144.
(18) (a) Kim, S.-J.; Kraus, F.; Fässler, T. F. *J. Am. Chem. Soc.* **2009**, *131*, 1469. (b) Kim, S.-J.; Fässler, T. F. *J. Solid State Chem.* **2009**, *182*, 778. (c) Kaltzoglou, A.; Ponou, S.; Fässler, T. F. *Eur. J. Inorg. Chem.* **2008**, 538. (d) Shimizu, T.; Imai, T.; Kume, S.; Sasaki, S.; Kaltzoglou, A.; Fässler, T. F. *Chem. Phys. Lett.* **2008**, *464*, 54.
(19) (a) *SHELXTL*; Bruker Analytical X-ray Instruments: Madison, WI, 1998. (b) Sheldrick, G. M. *Acta Crystallogr., Sect. A* **1990**, *46*, 467. (c) Sheldrick, G. M. *SHELXS-97, Program for the Solution of Crystal Structures*; Universität Göttingen: Göttingen, Germany, 1997. (d) Sheldrick, G. M. *SHELXL-97, Program for the Refinement of Crystal Structures*; Universität Göttingen: Göttingen, Germany, 1997.

***Table 2.*** Selected Interatomic Distances for $Na_5Zn_{2.28}Sn_{9.72(2)}$ (**I**) and $Na_5Hg_{2.39}Sn_{9.61(1)}$ (**II**)

| atom pair | | *d*/Å | atom pair | | *d*/Å | atom pair | | *d*/Å |
|---|---|---|---|---|---|---|---|---|
| | | | | **I** | | | | |
| Zn1 | Sn4 | 2.717(1) | Sn3/Zn | Sn5 | 2.838(1) | Na1 | Na3 | 3.450(7) |
| | Sn5 | 2.723(1) | | Sn4 | 2.841(1) | | Na2 | 3.746(7) |
| | Sn2 | 2.805(1) | | Sn1 | 2.907(1) | Na2 | Na3 | 3.428(7) |
| | Sn1 | 2.840(1) | | Sn3/Zn | 2.969(2) | | Na1 | 3.746(7) |
| Sn1 | Zn1 | 2.840(1) | Sn4 | Zn1 | 2.717(1) | Na3 | Na2 | 3.428(7) 2 × |
| | Sn5 | 2.868(1) | | Sn3/Zn | 2.841(1) | | Na1 | 3.450(7) 2 × |
| | Sn4 | 2.877(1) | | Sn2 | 2.863(1) | | | |
| | Sn3/Zn | 2.907(1) | | Sn1 | 2.877(1) | | | |
| Sn2 | Zn1 | 2.805(1) | Sn5 | Zn1 | 2.723(1) | | | |
| | Sn4 | 2.863(1) | | Sn3/Zn | 2.838(1) | | | |
| | Sn5 | 2.865(1) | | Sn2 | 2.865(1) | | | |
| | Sn2 | 2.986(1) | | Sn1 | 2.868(1) | | | |
| | | | | **II** | | | | |
| Hg1 | Sn4 | 2.818(1) | Sn3/Hg | Sn5 | 2.876(1) | Na1 | Na3 | 3.535(7) |
| | Sn5 | 2.828(1) | | Sn4 | 2.877(1) | | Na2 | 3.808(7) |
| | Sn2 | 2.868(1) | | Sn1 | 2.906(1) | Na2 | Na3 | 3.432(6) |
| | Sn1 | 2.993(1) | | Sn3/Hg | 3.025(1) | | Na1 | 3.808(7) |
| Sn1 | Sn5 | 2.884(1) | Sn4 | Hg1 | 2.818(1) | Na3 | Na2 | 3.432(6) 2 × |
| | Sn4 | 2.893(1) | | Sn2 | 2.866(1) | | Na1 | 3.535(7) 2 × |
| | Sn3/Hg | 2.906(1) | | Sn3/Hg | 2.877(1) | | | |
| | Hg1 | 2.993(1) | | Sn1 | 2.893(1) | | | |
| Sn2 | Sn5 | 2.862(1) | Sn5 | Hg1 | 2.828(1) | | | |
| | Sn4 | 2.866(1) | | Sn2 | 2.862(1) | | | |
| | Hg1 | 2.868(1) | | Sn3/Hg | 2.876(1) | | | |
| | Sn2 | 2.942(1) | | Sn1 | 2.884(1) | | | |

ments, the samples were diluted with diamond powder, finely ground in an agate mortar, and filled into glass capillaries which were sealed using a hot tungsten wire. Data collection took place in Debye−Scherrer mode, and the obtained patterns match perfectly with the theoretical diagrams calculated from single-crystal refinement data (Stoe WinXPow). The phases contained $\beta$-NaSn[23] (for **I**) and $\beta$-Sn (for **II**) as the main impurity.

**Electronic Structure Calculations.** Self-consistent band structure calculations for the hypothetical electron-richer and ordered phases "$Na_5M_{2+x}Sn_{10-x}$" [M = Zn (**I**), Hg (**II**), with $x = 0$] were performed with the linear-muffin-tin-orbital (LMTO) method using the LMTO-47[20] program code with the crystal orbital Hamilton population (COHP)[21] extension implemented. The *k*-space integration was performed by the tetrahedron method[22] on sets of 125 irreducible *k* points and a basis set with Na 3s/(3p,3d), Zn 4s/4p/3d, Hg 6s/6p/5d/(5f), and Sn-5s/5p/(5d/4f) (downfolded orbitals in parentheses). For space filling within the atomic sphere approximation, interstitial spheres (ES) were introduced in order to avoid too large overlaps of the atom-centered spheres. The empty spheres' positions and radii were calculated automatically within the limit of 18% overlap with any atom-centered spheres, and the WS radii [a.u.] Na 3.57−3.94, Sn 3.11−3.19, Zn 2.84, Hg 3.03, and ES = 1.66−2.23 were used. For bonding analyses, the energy contributions of all electronic states for selected bonds were evaluated with the COHP method. Integration over all filled states gives ICOHP values which measure the relative bond strengths. Negative COHP and ICOHP values indicate bonding interactions.

## 3. Results and Discussion

**Crystal Structures.** The isostructural and homologous compounds $Na_5M_{2+x}Sn_{10-x}$ (M = Zn, Hg) crystallize in an orthor-

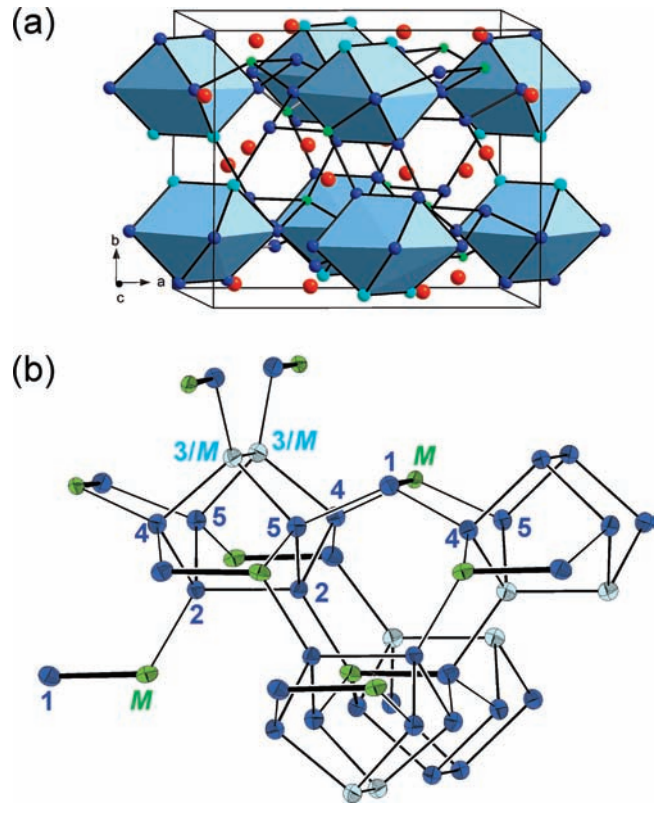


***Figure 1.*** (a) Projection of the unit cell of $Na_5M_{2+x}Sn_{10-x}$ along *c* with polyhedral representation of the realgar-type units. (b) Structural details emphasizing the connection of the realgar-type units. All atoms are drawn with thermal ellipsoids at 70% probability level. Sn, blue; Sn/M, teal; Na, red; M = Zn, Hg, green.

(20) (a) Andersen, O. K. *Phys. Rev. B* **1975**, *12*, 3060. (b) Anderson, O. K.; Jepsen, O. *Phys. Rev. Lett.* **1984**, *53*, 2571. (c) Krier, G.; Jepsen, O.; BurkhardtA.; Andersen, O. K. *TB-LMTO-ASA program, version 4.7*; Max Planck Institute for Solid State Research: Stuttgart, Germany, 1995.
(21) (a) Blöchl, P. E.; Dronskowski, R. *J. Phys. Chem.* **1993**, *97*, 8617. (b) Dronskowski, R. *Computational Chemistry of Solid State Materials*; Wiley-VCH: Weinheim/New York, 2005.
(22) Blöchl, P. E.; Jepsen, O.; Andersen, O. K. *Phys. Rev. B* **1994**, *49*, 16223.
(23) Mueller, W.; Volk, K. Z. *Naturforsch.* **1977**, *32B*, 709.

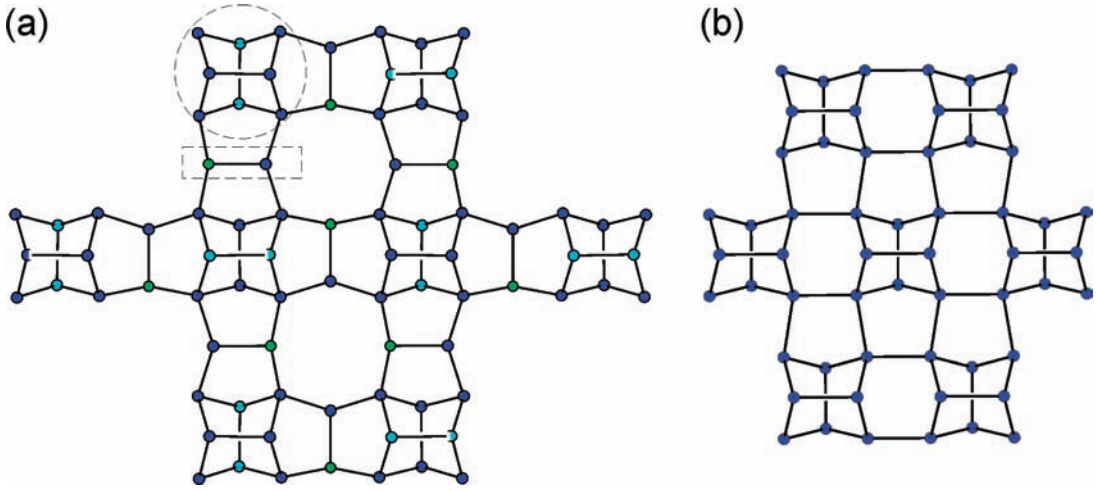


***Figure 2.*** (a) Two-dimensional structure details along the [010] direction of the $\{[M_xSn_{8-x}][MSn]_2\}$ framework in $Na_5M_{2+x}Sn_{10-x}$, showing the linkage of realgar-like $[M_xSn_{8-x}]$-by-[M−Sn] fragments indicated by a circle and a rectangle, respectively. (b) 2D polyanion $^2_\infty[Sn_8]^{4-}$ in the binary phase $NaSn_2$; here the realgar-type $[Sn_8]$ units are directly connected. Sn, blue; Sn/M, teal; M = Zn or Hg, green.

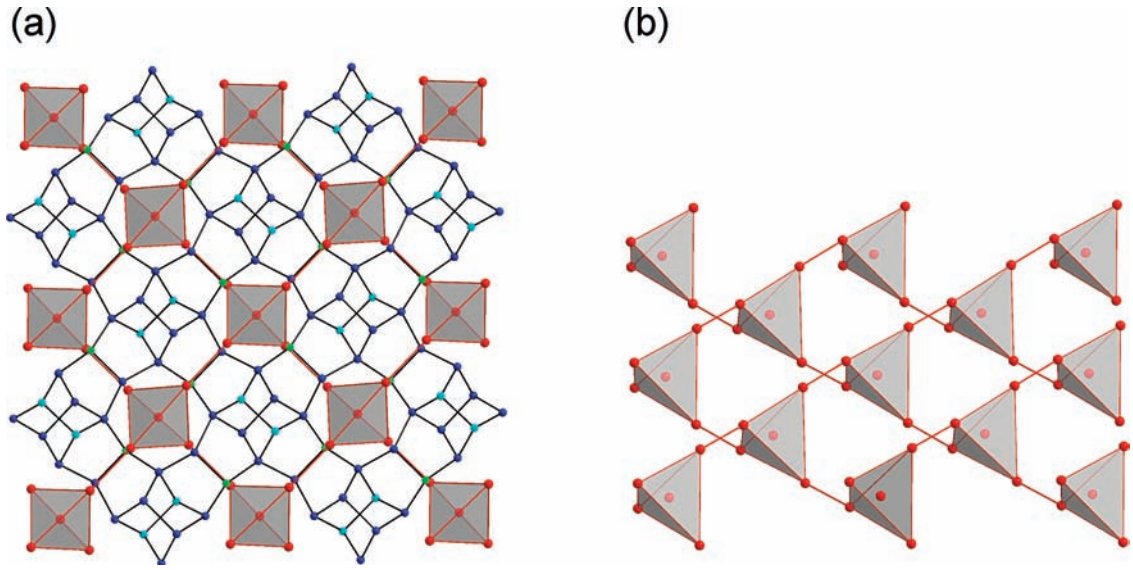


***Figure 3.*** (a) Interplay of anionic and cationic frameworks in $Na_5M_{2+x}Sn_{10-x}$. (b) 2D cationic array formed by interconnected $\{NaNa_4\}$ tetrahedra. Sn, blue; Sn/M, teal; M = Zn or Hg, green; Na, red.

hombic unit cell with the space group *Pbcn* (No. 60). The structure solution and refinement revealed that the new ternary phases crystallize with a complex 3D open framework of Sn and M atoms with Na cations located in the voids (Figure 1a). There are nine crystallographically independent atomic positions in the structures: one M-occupied position, five Sn positions of which one (Sn3) is mixed-occupied with roughly 15−20% Zn or Hg, and three Na-occupied sites of which one (Na3, site 4*c*) lies on a special position (Figure 1b).

The M−Sn framework of $Na_5M_{2+x}Sn_{10-x}$ (M = Zn, Hg) can be viewed as built from covalently bonded Sn and M atoms with distorted tetrahedral coordination environments. This sublattice contains two fundamental structural features: a realgar-like $[Sn_{8-x}M_x]$ unit and a dimeric fragment [M−Sn]. Both units are interconnected in the *ac* plane to form a sheet with a [M−Sn]:$[Sn_{8-x}M_x]$ ratio of 2:1, as shown in Figure 2a. The simple ABAB stacking of the anionic sheets allows further connections along the *b* direction *via* the [M−Sn] units, which themselves are tetrahedrally coordinated. In the resulting 3D framework, no direct connections between two equivalent units, cage or dimer, are observed. A related structure exists in the Zintl phase $NaSn_2$,[12] in which realgar-type $[Sn_8]$ units are directly coordinated to form a two-dimensional network, but with the Sn atom slabs separated by Na atoms (Figure 2b). Thus, the anionic sheet in $Na_5M_{2+x}Sn_{10-x}$ can be constructed from that of $NaSn_2$ (containing only $[Sn_8]$ units) by intercalating the [M−Sn] fragments between the $Sn_8$ units. Alternatively, the structure of $Na_5M_{2+x}Sn_{10-x}$ may be viewed as the result of the inclusion of the realgar-type unit $\{Sn_{8-x}M_x\}^{2x-}$ into the hypothetical phase "$Na_2MSn$", which can be regarded as a homologue of the well-characterized $Li_2ZnSn$[2] with a sphalerite-type $[ZnSn]^{2-}$ substructure. The partial Sn-by-M substitution in the realgar unit ($x = 1$) originates in this case from one unaccounted Na atom in the structure.

The Sn−Sn bond lengths (Table 2) range from 2.863(1) to 2.986(1) Å in **I** and from 2.862(1) to 2.942(1) Å in **II**, in agreement with those found in binary Na−Sn systems,[9] in which the Sn−Sn bonds are generally longer than the one in α-Sn (2.810 Å). The $ZnSn_4$ tetrahedron in **I** is distorted, and the Zn−Sn distances range from 2.717 to 2.840 Å. They compare

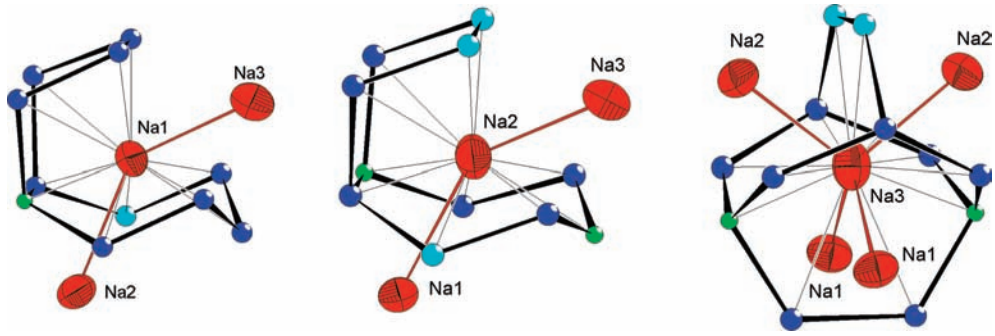


***Figure 4.*** Coordination of Na1, Na2, and Na3 atoms in the crystal structures of $Na_5M_{2+x}Sn_{10-x}$. The first coordination sphere cutoff has been set at 3.8 Å, and Na atoms are drawn at the 90% probability level. Sn, blue; Sn/M, teal; M = Zn or Hg, green; Na, red.

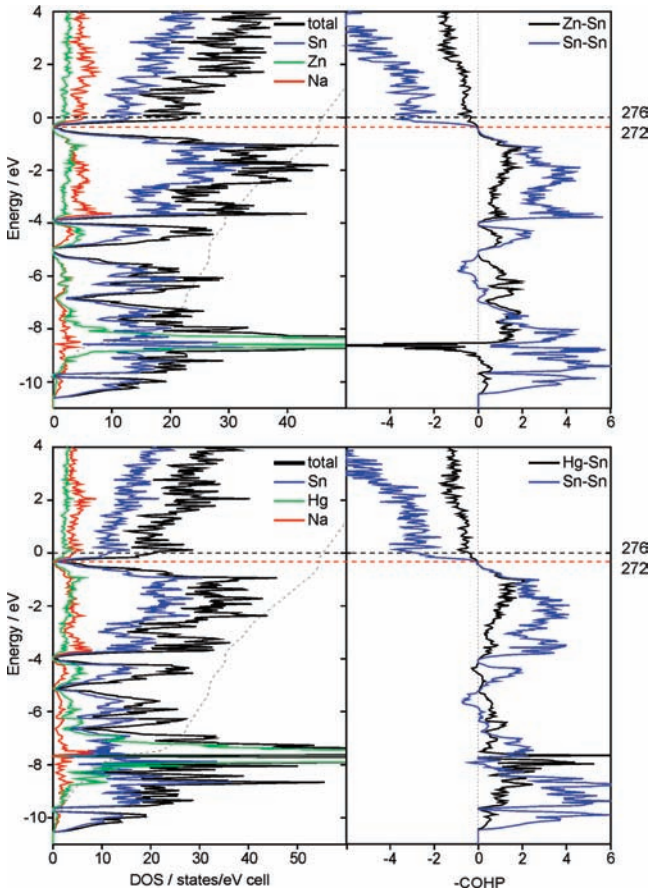


***Figure 5.*** Density of states and cumulative −COHP diagrams for $Na_5M_{2+x}Sn_{10-x}$ ($x = 0$): (top) M = Zn and (bottom) M = Hg. The Fermi energy ($E_F$) corresponds to the experimental 276 valence electrons/cell, and the vertical dotted line at the band gap (below $E_F$) marks the position of the Zintl phase limit of 272 valence electrons/cell.

well with the sum of the covalent radii of the atoms (1.40 Å + 1.33 Å = 2.73 Å).[24] An even stronger distortion is observed for the $HgSn_4$ tetrahedron in **II**, with Hg−Sn bond lengths between 2.818(1) and 2.993(1) Å; here, all but one of the Hg−Sn contacts are shorter than the sum of the covalent radii of Sn and Hg (1.40 Å + 1.50 Å = 2.90 Å). The unusual shrinkage of the Hg−Sn bonds with respect to the Sn−Sn distances is also observed in the mercury-substituted clathrate-I $A_8Hg_{4-x}Sn_{42+x}$ (A = K, Rb, Cs) characterized recently.[18c] The longest bonds in **I** are found between the Sn2 atoms of the $Sn_8$ realgar-like unit, with $d_{Sn2-Sn2} = 2.986(1)$ Å, and between Sn3 and the Zn atoms, with a distance of 2.969(2) Å; in **II**, the longest bonds of 3.025(1) Å are found between the two Sn3 positions, which are partially occupied with Hg, and thus correspond to an averaged Sn−Sn and Sn−Hg bond length.

Exclusively four-bonded (4b) framework atoms are common among group 14 element structures such as diamond and various clathrates.[25] Binary and ternary Zintl phases with exclusively 4b atoms in a polyanionic framework are also based on the two structure families. In NaTl-, $Li_2ZnSn$-, and AMSn (HH)-type phases, the electropositive atoms are located in the voids of the diamond-type structures. In the clathrates, the electropositive elements reside mainly inside the various cages.[26]

In the title compounds a new motif of a 4b network is realized. The larger voids are again occupied with Na atoms, and the cationic substructure forms a topologically interesting 2D network in the *ac* plane, which can be seen as interconnected $Na_4$ tetrahedra (Na 1 and Na2), centered by Na3 (Figure 3). The shortest Na−Na distances are found within the tetrahedra, with $d_{Na3-Na1} = 3.45$ Å (3.54 Å) and $d_{Na3-Na2} = 3.43$ Å (3.43 Å) for **I** (**II**). The interconnection between these $NaNa_4$ tetrahedra is realized through a longer Na1−Na2 distance of 3.75 Å in **I** and 3.81 Å in **II**. The three crystallographically different Na cations have distinct coordination environments, as shown in Figure 4, with interactions (<4 Å) between Na cations and the polyanionic framework (Table 2) ranging from 3.116(5) to 3.750(5) Å in **I** and from 3.148(3) to 3.794(5) Å in **II**.

**Electron Count.** Assuming a formal charge transfer from Na to the anionic network of Sn and M (Zn, Hg) according to the Zintl concept, $Na_5M_{2+x}Sn_{10-x}$ can be written as $(Na^+)_5[(4b\text{-}Sn^0)_{10-x}(4b\text{-}M^{2-})_{2+x}]$. For $x = 0.5$, the compound corresponds to an electron-precise Zintl phase with formally neutral Sn atoms and Zn or Hg atoms with a formal charge of 2−. In the hypothetical phase $Na_5M_2Sn_{10}$ ($x = 0$), the anionic unit would have to accommodate an additional electron per formula unit according to $(Na^+)_5[(4b\text{-}M^{2-})_2(4b\text{-}Sn^0)_{10}]\cdot(e^-)_1$. Alternatively, assuming the positive oxidation state for M of 2+, as found in, *e.g.*, zinc coordination compounds, leads to four three-connected Sn atoms (3b-$Sn^-$) per M atom. Consequently, for $x = 0$, the formula $(Na^+)_5(M^{2+})_2[(3b\text{-}Sn^-)_8(4b\text{-}Sn^0)_2]\cdot(e^-)_1$ results and has again an excess of one electron. *Binary* compounds in the tin-rich region of the phase diagram can compensate additional charge by increasing the coordination number of the tin atoms, as has been found for $NaSn_5$.[14] Therefore, nature uses partial

(24) (a) Pauling, L. *J. Am. Chem. Soc.* **1947**, *69*, 542. (b) Pauling, L. *Die Natur der chemischen Bindung*; Verlag Chemie: Weinheim, 1968.

(25) Guloy, A.; Ramlau, R.; Tang, Z.; Schnelle, W.; Baitinger, M.; Grin, Y. *Nature* **2006**, *443*, 320.

(26) Kovnir, K. A.; Shevelkov, A. V. *Russ. Chem. Rev.* **2004**, *73*, 923.

***Table 3.*** Average −ICOHP Values (eV/bond) of Different Interactions (Å) for $Na_5M_{2+x}Sn_{10-x}$ [$x = 0$, M = Zn (**I**), Hg (**II**)]

| | I | | | II | | |
|---|---|---|---|---|---|---|
| atom pair | distance | −ICOHP (max) | −ICOHP (at $E_F$) | distance | −ICOHP (max) | −ICOHP (at $E_F$) |
| Sn−Sn | 2.838−2.986 | 2.13 | 2.05 | 2.861−3.026 | 2.01 | 1.94 |
| Sn−M | 2.717−2.840 | 1.74 | 1.71 | 2.818−2.993 | 1.94 | 1.92 |
| Na−Sn | <3.8 | 0.18 | 0.18 | <3.8 | 0.18 | 0.17 |
| Na−M | <3.8 | 0.19 | 0.19 | <3.5 | 0.26 | 0.26 |

substitution by the electron-poorer M atoms at one of the Sn positions to optimize the electron count. The refined values for $x$ are 0.28(2) and 0.39(1) in **I** and **II**, respectively, which is less than the expected value of $x = 0.5$. A higher M content in the solid solutions, although possible, could not be confirmed by structure analyses. It is worth noting that the Sn3 position, which is partially substituted by M atoms, corresponds to the one without any direct contact to other M atoms. This can be understood by a minimization of electrostatic repulsion between neighboring M atoms, as illustrated also by the unusually long (Sn3/M)−(Sn3/M) distances (see above).

**Electronic Structure.** Band structure calculations were performed on phases with the idealized composition $Na_5M_2Sn_{10}$ (M = Zn or Hg) corresponding to $x = 0$. The calculated densities of states (DOS) are plotted in Figure 5 and are virtually identical for both the Zn and the Hg phases. The Fermi level cuts a region of finite DOS just above a deep minimum, which is located at about −0.36 eV below $E_F$. The band structure plot reveals that few bands cross the Fermi level at Γ (Supporting Information, Figures S1 and S2). The lower region in the DOS (between −7 and −9 eV) shows highly localized states (sharp spikes) that are essentially of Zn-3d or Hg-5d character. These Zn-3d and Hg-5d block bands are completely filled (Figures S1 and S2), and the resulting $d^{10}$ configuration leads to "pseudo-core" electrons or "pseudo-main-group" elements.[27] Valence s and p states are filled and are well separated at −4 to −10 and 0 to −4, respectively, with a pronounced 4s band for Zn at about −4.5 eV. The latter mainly interacts with Sn-5p orbitals. In both compounds the states originating from Sn-5s and -5p orbitals are also well separated, showing only little hybridization (Figure S1). Certainly, the charge transfer from Na to the framework is not complete, as can been seen from the amount of filled Na states in Figure 5. However, formal charge transfer to late transition metal ions with a $d^{10}$ configuration, like formal $Zn^{2-}$ or $Hg^{2-}$, are typically discussed for elements of the fifth and sixth periods.[28] In this sense, the electronic situation is rather similar to HH phases with a valence electron number of 18, such as MgCuSb and LiZnN, containing a sphalerite-type Cu−Sb and Zn−N network, respectively.[29]

The integrated DOS (IDOS) indicates that the electron count at the Fermi level is 276 valence electrons/formula unit (for $x = 0$), and at the DOS minimum there are 272 electrons/cell corresponding to $x = 0.5$, meaning that the compounds are then closed-shell Zintl phases. This also implies that the partial Zn (Hg)-for-Sn substitution, which occurs at one position, aims to optimize the electron count of the compound. Within the rigid band analyses, the electronic structure of the phases with the refined compositions $Na_5M_{2+x}Sn_{10-x}$ ($x \leq 0.5$) corresponds to a doped narrow-band-gap semiconductor, thereby meeting an important requirement of thermoelectric (TE) materials.[30] The slight but significant deviation from the optimum electron count which is observed in the refinement for both the Zn and the Hg phases may allow the control of the carrier concentration, which is critical for an improvement of the performance of TE materials, by tuning their transport properties.[31] Thus, the conducting properties of $Na_5M_{2+x}Sn_{10-x}$ will be affected by the valence electron count, and their TE properties may consequently be affected by their stoichiometry.

The COHP diagrams (Figure 5) indicate that the averaged Sn−Sn and Sn−M interactions are overall bonding below and antibonding above the pseudogap. The relative strength of the covalent bonding within the polyanionic framework is evidenced by the integrated crystal orbital Hamiltonian population (−ICOHP). In both the Zn and the Hg phases, the maximum values of the −ICOHP are achieved at the pseudogap (Table 3) and correspond to 2.13 and 2.01 eV/bond for Sn−Sn interactions and to 1.74 and 1.94 eV/bond for Sn−M interactions for **I** and **II**, respectively ($x = 0$). Replacement of Zn by Hg in $Na_5M_{2+x}Sn_{10-x}$ ($x = 0.5$) induces lower −ICOHP values for the Sn−Sn but not for the M−Sn bond. A very sharp antibonding spike between −9.0 and −8.5 eV is observed in the −COHP plot of the Zn phase (**I**). This may indicate some electrostatic repulsion between Sn-5s and Zn-3d orbitals; this phenomenon is not observed for the Hg phase (**II**) but it is also observed in hypothetical binary Sn−Zn phases.[32] In comparison, overlap populations of Na−Sn and Na−M interactions are weak, as indicated by the lower values of the −ICOHP between 0.18 and 0.19 eV/bond in **I** and between 0.18 and 0.26 eV/bond in **II**, which is in agreement with the predominantly ionic type of interactions. The strong covalent Sn−Sn and Sn−M bonds and the ionic Na interactions with the anionic framework are the main structure-directing forces and the key factors for the properties of these formal Zintl phases. An anionic framework with covalent bonds strong enough to produce a small band gap may lead to semiconducting behavior, which allows for a high Seebeck coefficient,[30] providing the "electron-crystal" system, whereas the cationic substructure with rattling atoms may provide the phonon-glass behavior.

## 4. Summary

Two novel phases with a new structure type containing exclusively four-fold-connected atoms have been synthesized, and their crystal structures were determined. The general

(27) Whangbo, M.-H.; Lee, C.; Köhler, J. *Angew. Chem., Int. Ed* **2006**, *45*, 7465.
(28) (a) Nesper, R. *Angew. Chem., Int. Ed. Engl.* **1991**, *30*, 789. (b) Sommer, A. *Nature* **1943**, *152*, 215. (c) Karpov, A.; Nuss, J.; Wedig, U.; Jansen, M. *J. Am. Chem. Soc.* **2004**, *126*, 14123. (d) Jansen, M. *Solid State Sci.* **2005**, *7*, 1464. (e) Karpov, A.; Konuma, M.; Jansen, M. *Chem. Commun.* **2006**, *8*, 838.
(29) (a) Köhler, J.; Whangbo, M.-H. *Solid State Sci.* **2008**, *10*, 444. (b) Offernes, L.; Ravindran, P.; Kjekshus, A. *J. Alloys Compd.* **2007**, *439*, 37.
(30) Snyder, G. J.; Toberer, E. S. *Nat. Mater.* **2008**, *7*, 105.
(31) (a) Gascoin, F.; Ottensmann, S.; Stark, D.; Haile, S. M.; Snyder, G. J. *Adv. Funct. Mater.* **2005**, *15*, 1860. (b) Kauzlarich, S. M.; Brown, S. R.; Snyder, G. J. *Dalton Trans.* **2007**, 2099.
(32) von Appen, J.; Dronskowski, R.; Hack, K. *J. Alloys Compd.* **2004**, *379*, 110.

chemical formula $Na_5M_{2+x}Sn_{10-x}$ (M = Zn, Hg) corresponds to a charge-balanced Zintl phase (valence compound) when $x = 0.5$. The formulation of the phases as $(Na^+)_5(M^{2-})_{2+x}(Sn^0)_{10-x}$ with transition metal *anions* is manifested by the fact that the frontier orbitals of these compounds are not described by the transition metal *n*d orbitals but by the transition metal $(n+1)$sp orbitals. The structures are related to the half-Heusler alloys, as they are intermediate between unfilled and stuffed diamond structures. The usually large values of the thermal conductivity $\kappa_L$ in the half-Heusler alloys have proven to be the major obstruction for application of these materials in thermoelectric devices.[5,6] The ternary Zintl phases $Na_5M_{2+x}Sn_{10-x}$ show similar chemical and electronic features, but, due to their cage-like structure and their complex unit cells, a dip in $\kappa_L$ may be possible. Efforts to produce phase-pure samples necessary for physical property investigations are ongoing.

**Acknowledgment.** We thank Dr. A. Schier for the revision of the manuscript.

**Supporting Information Available:** X-ray crystallographic files in CIF format for $Na_5Zn_{2.3}Sn_{9.7(2)}$ and $Na_5Hg_{2.4}Sn_{9.6(1)}$; tables with all bond lengths, atomic positions, and anisotropic displacement parameters as well as band dispersion and DOS plots including partial DOS for "$Na_5Zn_2Sn_{10}$" and "$Na_5Hg_2Sn_{10}$". This material is available free of charge via the Internet at http://pubs.acs.org.

JA902664C